

# Solid-State Reactions Occurring during the Synthesis of CaTiO<sub>3</sub>–NdAlO<sub>3</sub> Perovskite Solid Solutions

Bostjan Jancar,\* Matjaz Valant, and Danilo Suvorov

Jožef Stefan Institute, Jamova 39, 1000 Ljubljana, Slovenia

Received October 8, 2003. Revised Manuscript Received January 19, 2004

The X-ray powder-diffraction technique was used to investigate the solid-state reaction paths to the 0.7CaTiO<sub>3</sub>–0.3NdAlO<sub>3</sub> perovskite solid solution. The results show that the perovskite phases CaTiO<sub>3</sub> and NdAlO<sub>3</sub> are formed prior to the solid solution, regardless of the combination of oxide powders used as reagents. The two perovskites subsequently react to form a solid solution at temperatures above 1200 °C. The reaction between CaTiO<sub>3</sub> and NdAlO<sub>3</sub> was studied using a diffusion couple, which revealed that the slower kinetics of incorporation of the Al into the forming solid solution results in the formation of an intermediate phase based on hexaluminate CaAl<sub>12</sub>O<sub>19</sub>. The presence of such inclusions results in the formation of defects in the perovskite matrix phase, which adversely affects the dielectric losses of the sintered ceramics based on the 0.7CaTiO<sub>3</sub>–0.3NdAlO<sub>3</sub> solid solution. To minimize the concentration of CaAl<sub>12</sub>O<sub>19</sub>-based inclusions, a thorough calcination procedure with intermediate homogenizations needs to be conducted at temperatures above 1300 °C.

## Introduction

Perovskite solid solutions based on the CaTiO<sub>3</sub>–REAlO<sub>3</sub> (RE = La, Nd, Sm) systems were identified as promising candidates for the synthesis of mid-permittivity-class microwave dielectric ceramics<sup>1</sup> and have thus received much attention in the recent scientific literature.<sup>2–7</sup> A highly positive temperature coefficient of resonant frequency ( $\tau_f = +800$  ppm/K), which is inherent to pure CaTiO<sub>3</sub>, is effectively suppressed by the addition of 30–35 mol % of REAlO<sub>3</sub>. Apart from temperature-stable resonant frequencies the ceramics based on solid solutions with such compositions exhibit high permittivities ( $\epsilon_r > 40$ ) and high Q-value ( $Q_{xf} > 40000$  GHz), which make them attractive for uses in rapidly developing telecommunication technologies. In the CaTiO<sub>3</sub>–REAlO<sub>3</sub> family, the CaTiO<sub>3</sub>–NdAlO<sub>3</sub>-based ceramics are already being used for the commercial production of base-station microwave dielectric resonators in wireless-communication networks.

In the scope of our investigations of the (1–*x*)CaTiO<sub>3</sub>–*x*NdAlO<sub>3</sub> system we showed that the two perovskites form solid solutions across the entire compositional range. The  $\epsilon_r$  and the  $\tau_f$  of the ceramics based on these

solid solutions decrease with the increase in *x* whereas the Q-value increases.<sup>2,5</sup> The ceramics based on the solid solution with *x* = 0.3 exhibit a temperature-stable resonant frequency ( $\tau_f = +3$  ppm/K), a high permittivity ( $\epsilon_r = 45$ ), and a  $Q_{xf}$  which can be tuned up to 45000 GHz with the proper choice of processing conditions.<sup>5</sup> Such microwave dielectric properties make ceramics based on the 0.7CaTiO<sub>3</sub>–0.3NdAlO<sub>3</sub> solid solution suitable for the production of commercial dielectric resonators. Further investigations into the crystal structure and the microstructure of 0.7CaTiO<sub>3</sub>–0.3NdAlO<sub>3</sub> ceramics revealed four distinct microstructural features<sup>5</sup>: antiphase boundaries, twin boundaries, and two types of inclusions rich in Al, spinel-MgAl<sub>2</sub>O<sub>4</sub>, and hexaluminate based on CaAl<sub>12</sub>O<sub>19</sub>. The twin and antiphase boundaries are formed as a result of the symmetry-breaking structural phase transitions, which occur during cooling from the sintering temperature. The formation of the spinel inclusions is a consequence of the Mg-based impurities, which are probably brought into the system with the CaCO<sub>3</sub>. The origin of the CaAl<sub>12</sub>O<sub>19</sub>-based inclusions, however, was not elucidated.

The presence of the inclusions in the microstructure necessarily influences the microwave dielectric properties of the ceramics. Therefore, understanding the mechanism of the formation of these Al-rich hexaluminate inclusions is of crucial importance in controlling the dielectric properties of 0.7CaTiO<sub>3</sub>–0.3NdAlO<sub>3</sub> microwave ceramics. The objective of this study was to investigate the solid-state reaction mechanism that occurs during the formation of the 0.7CaTiO<sub>3</sub>–0.3NdAlO<sub>3</sub> solid solution to determine the origin of the CaAl<sub>12</sub>O<sub>19</sub>-based inclusions.

## Experimental Section

Stoichiometric amounts of reagent-grade powders of CaCO<sub>3</sub> (Johnson Matthey 99.95%), TiO<sub>2</sub> (Johnson Matthey >99%),

\* To whom correspondence should be addressed. E-mail: bostjan.jancar@ijs.si.

(1) Seiichiro, H.; Nobuyoshi, F.; Sehinichi, E.; Toyomi, N. Japanese Patent, 2625074, 1994.

(2) Jancar, B.; Suvorov, D.; Valant, M. *J. Mater. Sci. Lett.* **2001**, *20*, 71.

(3) Kim, M. H.; Nahm, S.; Choi, C. H.; Lee, H. J.; Park, H. M. *Jpn. J. Appl. Phys.* **2002**, *41*, 717.

(4) Jancar, B.; Suvorov, D.; Valant, M. *Key. Eng. Mater.* **2002**, *206–2*, 1289.

(5) Jancar, B.; Suvorov, D.; Valant, M.; Drazic, G. *J. Eur. Ceram. Soc.* **2003**, *23* (9), 1391.

(6) Zheng, H.; Bagshaw, H.; Csete de Gyorgyfalva, G.D.C.; Reaney, I. M.; Ubbelohde, R.; Yarwood, J. *J. Appl. Phys.* **2003**, *94* (5), 2948.

(7) Neneasheva, E. A.; Mudroliubova, L. P.; Karmenko, N. F. *J. Eur. Ceram. Soc.* **2003**, *23* (14), 2443.

$\text{Nd}_2\text{O}_3$  (Johnson Matthey 99.99%), and  $\text{Al}_2\text{O}_3$  (Johnson Matthey 99.99%) were homogenized under ethanol in an yttria-stabilized-zirconia ball-mill using balls with a diameter of 3 mm. Since the  $\text{Nd}_2\text{O}_3$  powder is strongly hygroscopic, it was dried for 12 h at 850 °C prior to weighing. After homogenization the mixture was dried using a rotary evaporator, pressed into pellets under a pressure of 10 MPa, and fired at several temperatures between 500 and 1400 °C. To study the solid-state reactions that occur at a certain temperature, the reaction mixture was quenched to room temperature after each firing. The phase composition was analyzed using X-ray powder-diffraction analysis with a Philips PW 1710 X-ray powder diffractometer and  $\text{Cu K}\alpha$  radiation. Thermal analyses (TG and DTA) were performed with a Netzsch STA 409 thermal analysis system in an air atmosphere using an  $\text{Al}_2\text{O}_3$  crucible. Evolved-gas analysis (EGA) was carried out on  $\text{CO}_2^+$ ,  $\text{H}_2\text{O}^+$ , and  $\text{OH}^+$  fragments with a Balzers Thermostat GSD 300T quadrupole mass spectrometer.

Three additional reaction paths were examined by the use of alternative reagents such as  $\text{CaTiO}_3$  and  $\text{NdAlO}_3$ .  $\text{CaTiO}_3$  was obtained by prereacting a homogenized mixture of  $\text{CaCO}_3$  and  $\text{TiO}_2$  at 1200 °C whereas  $\text{NdAlO}_3$  was prepared by prereacting  $\text{Nd}_2\text{O}_3$  and  $\text{Al}_2\text{O}_3$  at 1600 °C. In one case a stoichiometric mixture of the perovskites  $\text{CaTiO}_3$  and  $\text{NdAlO}_3$  was fired at several temperatures between 500 and 1400 °C. In the second case  $\text{CaTiO}_3$  was fired in the same temperature range with stoichiometric amounts of  $\text{Nd}_2\text{O}_3$  and  $\text{Al}_2\text{O}_3$  whereas in the third case  $\text{NdAlO}_3$  was fired with stoichiometric amounts of  $\text{CaCO}_3$  and  $\text{TiO}_2$ .

For the purpose of studying the reaction between the pre-reacted  $\text{CaTiO}_3$  and  $\text{NdAlO}_3$  a diffusion couple was prepared. A pellet of the  $\text{NdAlO}_3$  pre-sintered at 1600 °C was embedded in a powder of  $\text{CaTiO}_3$  and isostatically pressed under 700 MPa. After firing at 1350 °C, the diffusion couple was polished and the interface analyzed with a JEOL JSM-5800 scanning electron microscope (SEM) equipped with the Oxford Link-Isis energy-dispersive X-ray analysis systems (EDS).

The lattice parameters of the perovskite solid solution were calculated by the whole powder-pattern decomposition method,<sup>8</sup> using the computer program TOPAS-R (Bruker AXS, Karlsruhe, Germany).

The microwave dielectric measurements of the ceramic samples sintered at 1350 °C were performed with an HP 8719C network analyzer using a cavity-reflection method. The  $Q$ -values of the  $\text{TE}_{010}$  resonance mode were determined from a Smith chart by analyzing the  $S_{11}$  parameter as proposed by Kajfez and Hwan.<sup>9</sup> The permittivities were calculated from the same resonance frequency using the Itoh-Rudokas model.<sup>10</sup>

## Results and Discussion

The X-ray analysis of the commercial reagent powders used for the synthesis of the  $\text{CaTiO}_3$ – $\text{NdAlO}_3$  solid solutions revealed that the dried  $\text{Nd}_2\text{O}_3$  powder consisted of two polymorphs, hexagonal A- $\text{Nd}_2\text{O}_3$  and a small amount of cubic C- $\text{Nd}_2\text{O}_3$ . The  $\text{TiO}_2$  powder contained some anatase phase in addition to rutile; the  $\text{CaCO}_3$  powder consisted of pure calcite; and the  $\text{Al}_2\text{O}_3$  powder was pure  $\alpha$ - $\text{Al}_2\text{O}_3$ . After the homogenization the mixture of these powders also contained some  $\text{Nd}(\text{OH})_3$ , which suggests that the  $\text{Nd}_2\text{O}_3$  reacts with water contained in the alcohol (Figure 1). Similar mixtures of reagent powders were used to synthesize the  $\text{CaTiO}_3$ – $\text{NdAlO}_3$  solid solutions in the majority of our previous experiments.<sup>2,4,5</sup>

To determine the temperatures marking the onset of solid-state reactions among the reagent powders, we performed a thermal analysis. From the DTA and TG

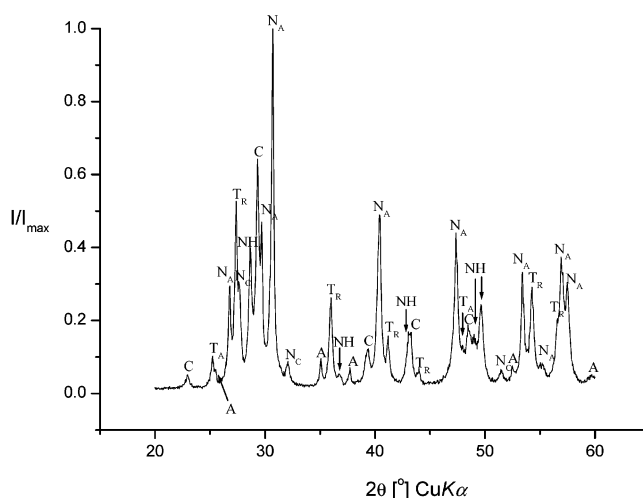


**Figure 1.** X-ray diffraction pattern of the  $\text{CaCO}_3$ ,  $\text{TiO}_2$ ,  $\text{Nd}_2\text{O}_3$ , and  $\text{Al}_2\text{O}_3$  reaction mixture after homogenization. (C =  $\text{CaCO}_3$ ,  $T_A$  =  $\text{TiO}_2$ -anatase,  $T_R$  =  $\text{TiO}_2$ -rutile,  $N_C$  = C- $\text{Nd}_2\text{O}_3$ ,  $N_A$  = A- $\text{Nd}_2\text{O}_3$ , NH =  $\text{Nd}(\text{OH})_3$ , A =  $\text{Al}_2\text{O}_3$ ).

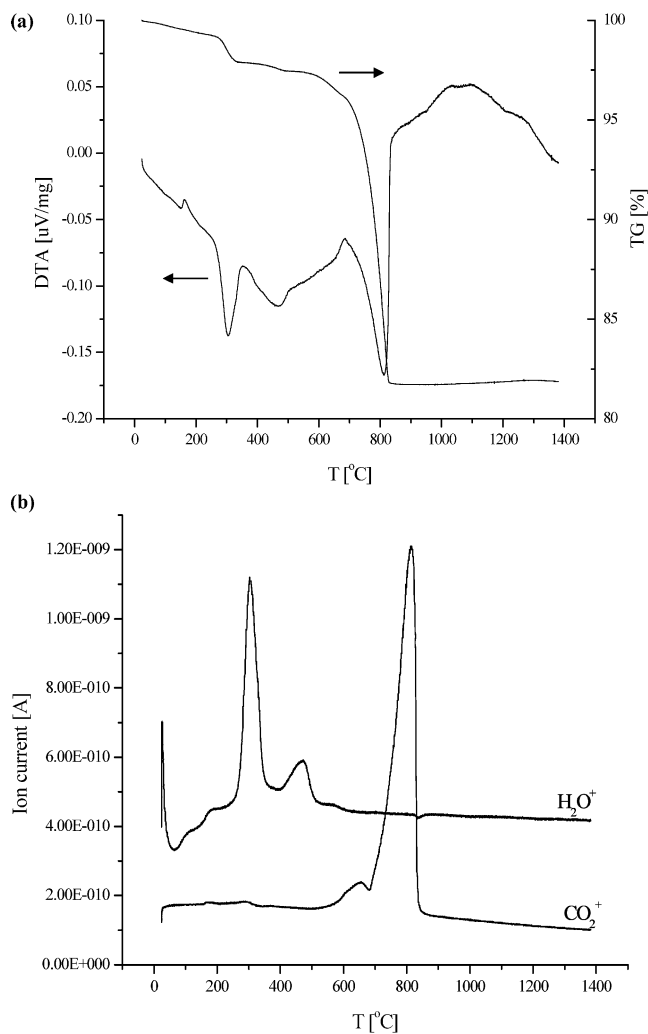


**Figure 2.** (a) TG, DTA, and (b) EGA curves of the  $\text{CaCO}_3$ ,  $\text{TiO}_2$ ,  $\text{Nd}_2\text{O}_3$ , and  $\text{Al}_2\text{O}_3$  reaction mixture recorded in the temperature range 20–1400 °C with a heating rate at 5 K/min.

curves shown in Figure 2a it can be seen that the first reactions to occur in the range between room temperature and 811 °C are endothermic, and they are accompanied by a weight loss. According to the EGA curve, shown in Figure 2b, the two endothermic reactions

(8) Pawley, G. S. *J. Appl. Crystallogr.* **1981**, *14*, 357.

(9) Kajfez, D.; Hwan, E. J. *IEEE Trans. MTT* **1984**, *MTT-32*, 666.

(10) Itoh, T.; Rudokas, R. S. *IEEE Trans. MTT* **1977**, *MTT-8*, 52.

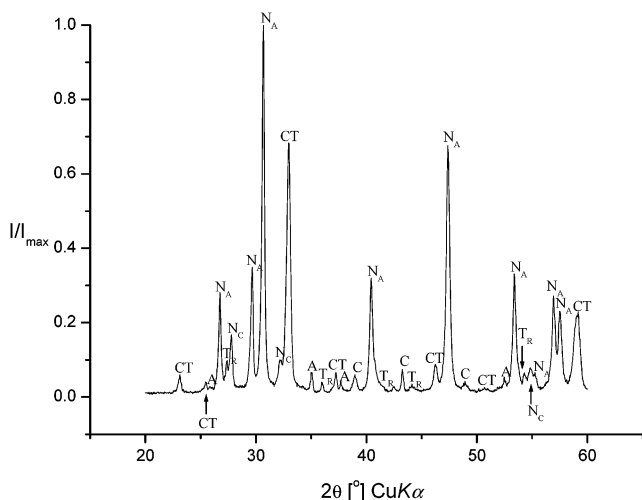


**Figure 3.** X-ray diffraction pattern of the CaCO<sub>3</sub>, TiO<sub>2</sub>, Nd<sub>2</sub>O<sub>3</sub>, and Al<sub>2</sub>O<sub>3</sub> reaction mixture after firing at 850 °C/2 h. (CT = CaTiO<sub>3</sub>, C = CaO).

which occur at 304 and 466 °C result in the release of H<sub>2</sub>O from the reaction mixture, and a reaction at 811 °C results in the release of CO<sub>2</sub>. The two peaks indicating the loss of water can be attributed to the two-stage decomposition mechanism of Nd(OH)<sub>3</sub>, which was proposed by Klevtsov.<sup>11</sup> According to this mechanism, Nd(OH)<sub>3</sub> decomposes to Nd<sub>2</sub>O<sub>3</sub> and water vapor via the intermediate compound NdOOH. Inspection of the CO<sub>2</sub><sup>+</sup> peak in the EGA curve reveals that at a heating rate of 5 K/min the decomposition of the CaCO<sub>3</sub> in the reaction mixture takes place in the temperature range 650–850 °C, which is in accordance with the decomposition of pure CaCO<sub>3</sub>. Furthermore, the DTA curve exhibits a broad exothermic peak between 850 and 1300 °C. The exothermic effect can be attributed to the solid-state reactions among the reagent powders.

The X-ray diffraction analysis of the reaction mixture after firing at 850 °C reveals the presence of CaTiO<sub>3</sub> (Figure 3). On the basis of this result, we can conclude that apart, from the decomposition of Nd(OH)<sub>3</sub> and CaCO<sub>3</sub>, the formation of CaTiO<sub>3</sub> is the only reaction that occurs up to 850 °C. The exothermic effect of this reaction is masked by the endothermic decomposition of the CaCO<sub>3</sub> and therefore does not show in the DTA curve. The formation of the CaTiO<sub>3</sub> below 850 °C can proceed via two possible solid-state reactions, which may occur simultaneously. The TiO<sub>2</sub> powder can either react directly with CaCO<sub>3</sub> powder, thus causing its decomposition, or the reaction takes place between TiO<sub>2</sub> and the CaO released after the thermal decomposition of CaCO<sub>3</sub>. Such a two-stage mechanism where a carbonate is first thermally decomposed to CO<sub>2</sub> and an oxide which subsequently reacts with another oxide to form a new compound was already proposed for the case of the solid-state synthesis of BaTiO<sub>3</sub> from BaCO<sub>3</sub> and TiO<sub>2</sub>.<sup>12</sup>

The presence of the CaO in the reaction mixture after firing at 850 °C for 2 h, however, indicates that the thermal decomposition of CaCO<sub>3</sub> proceeds faster than the formation of CaTiO<sub>3</sub> (Figure 3). Up to this temperature the Nd<sub>2</sub>O<sub>3</sub> and Al<sub>2</sub>O<sub>3</sub> powders remain unreacted.

Firing the reaction mixture at temperatures in the range between 1000 and 1200 °C leads to additional

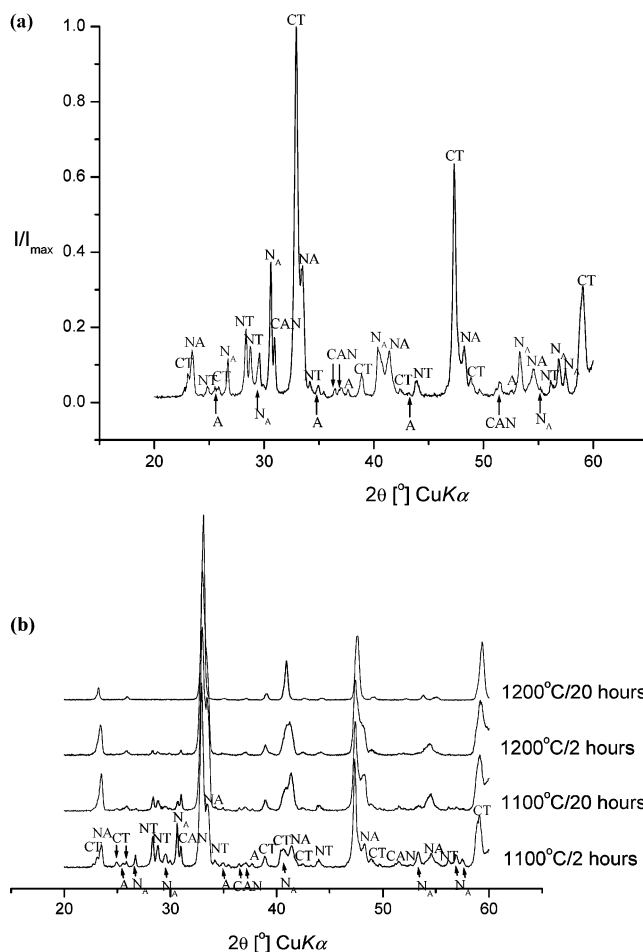


**Figure 4.** X-ray diffraction pattern of the CaCO<sub>3</sub>, TiO<sub>2</sub>, Nd<sub>2</sub>O<sub>3</sub>, and Al<sub>2</sub>O<sub>3</sub> reaction mixture after firing at (a) 1000 °C/2 h and (b) at 1100 °C and 1200 °C. (NA = NdAlO<sub>3</sub>, NT = Nd<sub>2</sub>TiO<sub>5</sub>, CAN = CaNdAl<sub>3</sub>O<sub>7</sub>).

solid-state reactions that result in the formation of three new phases: Nd<sub>2</sub>TiO<sub>5</sub>, CaNdAl<sub>3</sub>O<sub>7</sub>, and NdAlO<sub>3</sub>. However, above 1100 °C the Nd<sub>2</sub>TiO<sub>5</sub> and CaNdAl<sub>3</sub>O<sub>7</sub> react, forming the perovskites CaTiO<sub>3</sub> and NdAlO<sub>3</sub> (Figure 4).

According to the X-ray spectra shown in Figure 4b, the final reaction, which leads to the formation of the 0.7CaTiO<sub>3</sub>-0.3NdAlO<sub>3</sub> solid solution, takes place between the two perovskites CaTiO<sub>3</sub> and NdAlO<sub>3</sub> at temperatures above 1200 °C.

With the use of alternative reagents, we examined three additional paths to the 0.7CaTiO<sub>3</sub>-0.3NdAlO<sub>3</sub> solid solution. When prereacted powders of CaTiO<sub>3</sub> and NdAlO<sub>3</sub> are used, the solid solution forms by a direct reaction between the two perovskites above 1200 °C, without the intermediate formation of Nd<sub>2</sub>TiO<sub>5</sub> and CaNdAl<sub>3</sub>O<sub>7</sub> at lower temperatures (Figure 5a). Similarly, the use of prereacted NdAlO<sub>3</sub> and stoichiometric amounts of CaCO<sub>3</sub> and TiO<sub>2</sub> results in the two perovskite phases (Figure 5b), which subsequently react into a solid solution as shown in Figure 5a. However, when CaTiO<sub>3</sub> is used in combination with stoichiometric amounts of Nd<sub>2</sub>O<sub>3</sub> and Al<sub>2</sub>O<sub>3</sub>, the situation resembles the case when CaCO<sub>3</sub>, TiO<sub>2</sub>, Nd<sub>2</sub>O<sub>3</sub>, and Al<sub>2</sub>O<sub>3</sub> are used as starting reagents. At 1000 °C (Figure 5c) the two intermediate phases Nd<sub>2</sub>TiO<sub>5</sub> and CaNdAl<sub>3</sub>O<sub>7</sub> form and subsequently react to give CaTiO<sub>3</sub> and NdAlO<sub>3</sub>, which then react to form a solid solution at temperatures above 1200 °C, in accordance with Figure 4.

(11) Klevtsov, V.; Sheina, L. P. *Inorg. Mater. (USSR)* **1965**, *1*, 2006.

(12) Beauger, A.; Mutin, J.; Niepce, J. *J. Mater. Sci.* **1983**, *18*, 3041.



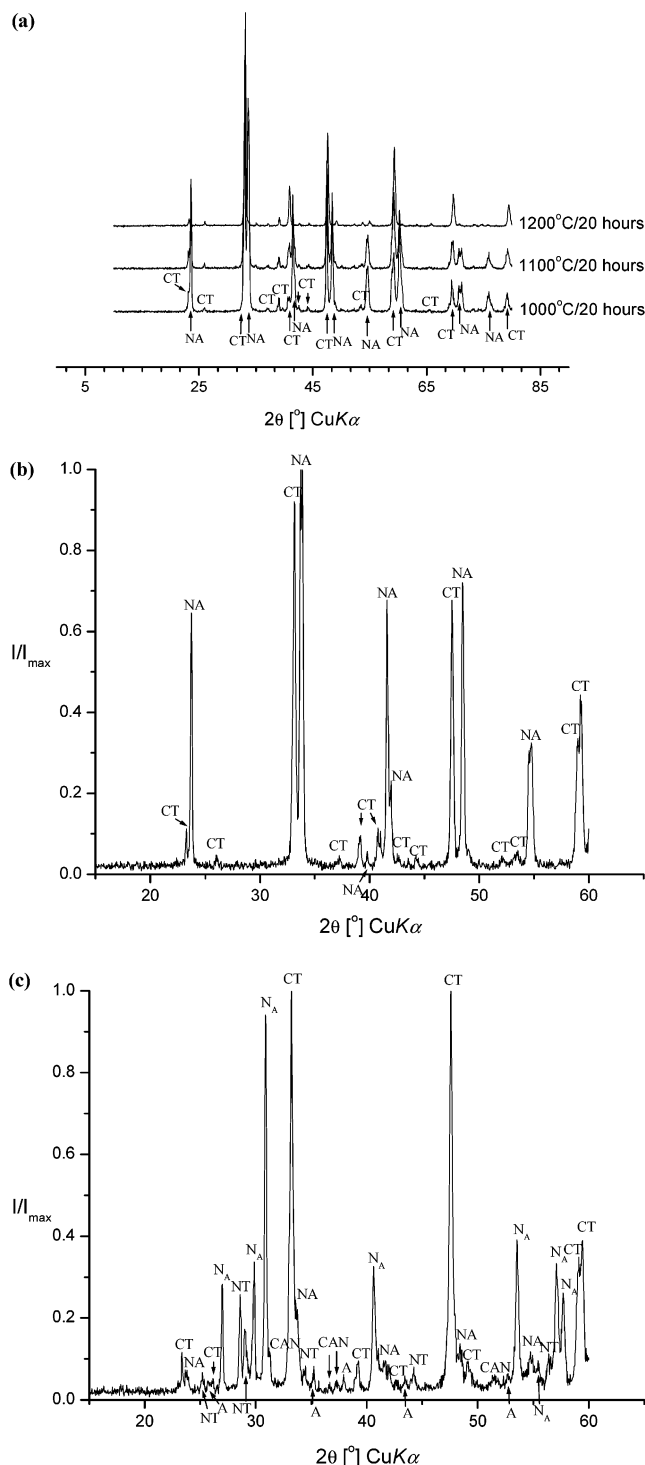


**Figure 5.** X-ray diffraction pattern of (a) a  $\text{CaTiO}_3$  and  $\text{NdAlO}_3$  mixture after firing at different temperatures, (b) a  $\text{CaCO}_3$ ,  $\text{TiO}_2$ , and  $\text{NdAlO}_3$  mixture after firing at 1000 °C/2 h, and (c) a  $\text{CaTiO}_3$ ,  $\text{Nd}_2\text{O}_3$ , and  $\text{Al}_2\text{O}_3$  mixture after firing at 1000 °C/2 h.

These findings suggest that the intermediate phases  $\text{Nd}_2\text{TiO}_5$  and  $\text{CaNdAl}_3\text{O}_7$  only form when free  $\text{Nd}_2\text{O}_3$  and  $\text{Al}_2\text{O}_3$  are present in the reaction mixture. In such a case several parallel reactions take place at temperatures between 1000 and 1200 °C. Apart from reacting with each other to form  $\text{NdAlO}_3$ , the two oxides  $\text{Nd}_2\text{O}_3$  and  $\text{Al}_2\text{O}_3$  react with either free  $\text{CaO}$  and  $\text{TiO}_2$  or with  $\text{CaTiO}_3$  to form  $\text{Nd}_2\text{TiO}_5$  and  $\text{CaNdAl}_3\text{O}_7$ . Furthermore,  $\text{Nd}_2\text{TiO}_5$  and  $\text{CaNdAl}_3\text{O}_7$  react, forming the perovskites  $\text{CaTiO}_3$  and  $\text{NdAlO}_3$ .

Inspection of the X-ray diffraction spectrum shown in Figure 4b reveals that in the early stages of the firing process the concentration of  $\text{Nd}_2\text{TiO}_5$  and  $\text{CaNdAl}_3\text{O}_7$  increases, whereas in the later stages it decreases. This confirms the transient nature of the two phases. With a high concentration of  $\text{Nd}_2\text{O}_3$  and  $\text{Al}_2\text{O}_3$ , which is the case in the early stages of firing, the formation of  $\text{Nd}_2\text{TiO}_5$  and  $\text{CaNdAl}_3\text{O}_7$  proceeds faster than the reaction between them that leads to  $\text{CaTiO}_3$  and  $\text{NdAlO}_3$ . However, the reverse is true for the later stages of the reaction when the majority of the  $\text{Nd}_2\text{O}_3$  and  $\text{Al}_2\text{O}_3$  is consumed.

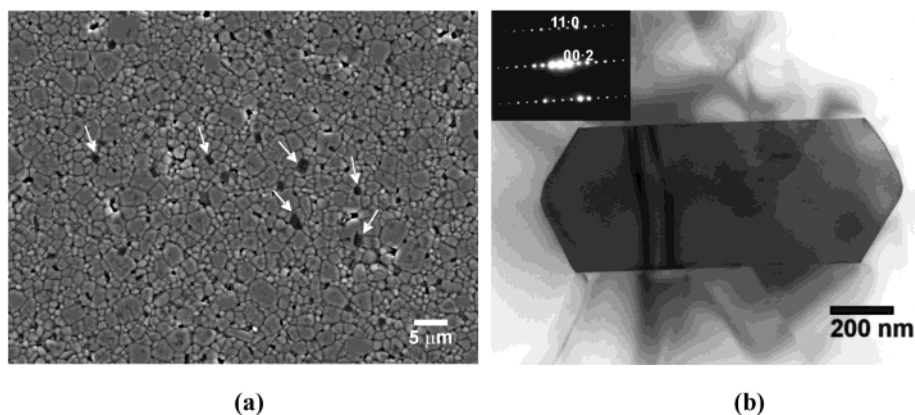
From these results, summarized in Table 1, we concluded that the reaction between  $\text{CaTiO}_3$  and  $\text{NdAlO}_3$  is common to all four alternatives of the reagent powders used for the synthesis of the  $0.7\text{CaTiO}_3-0.3\text{NdAlO}_3$  solid solution.

Figure 6 shows the microstructure of the sintered  $0.7\text{CaTiO}_3-0.3\text{NdAlO}_3$  ceramics. Apart from the matrix-phase grains the secondary-phase inclusions with sizes ranging from 0.5 to 3  $\mu\text{m}$  are clearly visible. In the course of our previous investigations it was determined that these inclusions are based on hexaluminate  $\text{CaAl}_{12}\text{O}_{19}$ .<sup>5</sup> Since the presence of these hexaluminate inclusions in the microstructure of the sintered ceramics seems to be unaffected by the choice of the reagent powders or the sintering conditions, we further concluded that their source must be the reaction between the two perovskites. To study this reaction in more detail, we prepared several diffusion couples.

According to the X-ray spectra shown in Figure 4b, a temperature of 1200 °C is sufficient for the reaction between  $\text{CaTiO}_3$  and  $\text{NdAlO}_3$  to occur. However, the kinetics of the reaction at this temperature is relatively slow. With the intention to follow the reaction on a more acceptable time scale, we fired the diffusion couples at 1350 °C. The interface area of the  $\text{CaTiO}_3$ - $\text{NdAlO}_3$  diffusion couple fired at 1350 °C for 6 h is shown in Figure 7. The reaction layer that forms between  $\text{CaTiO}_3$  and  $\text{NdAlO}_3$  consists of at least two phases: (1) a *continuous phase* filling the area between the  $\text{CaTiO}_3$  and the  $\text{NdAlO}_3$ , and (2) *discrete particles*, segregated along the  $\text{NdAlO}_3$  side. Semiquantitative EDS analysis shows that the discrete particles are rich in Al. Furthermore, EDS analysis reveals that in the continuous phase the concentration of Nd is higher than the concentration of Al, and the concentration of Ti is higher than the concentration of Ca. A clearer insight into the reaction between  $\text{CaTiO}_3$  and  $\text{NdAlO}_3$  is offered when the diffusion couple is fired for a longer period of time. Apart from the increase in the reaction-layer thickness associated with the nucleation of a higher concentration of Al-rich particles, the extended firing time results in the growth of the *discrete particles* (Figure 8). After a certain time the growing particles coalesce, thus forming Al-rich phase regions in the reaction layer. In the diffusion couple fired at 1350 °C for 100 h the average size of these phase regions exceeds 10  $\mu\text{m}$ , which allows a more selective EDS analysis. The results of such an SEM/EDS analysis are comparable to the results of the TEM/EDS analysis performed on the  $\text{CaAl}_{12}\text{O}_{19}$ -based inclusions found in the  $0.7\text{CaTiO}_3-0.3\text{NdAlO}_3$  ceramics. These findings and the similarity of the morphology lead us to a conclusion that the particles formed in the

**Table 1. Solid-State Reactions Occurring during the Synthesis of the 0.7CaTiO<sub>3</sub>-0.3NdAlO<sub>3</sub> Solid Solution**

Reagent powders	CaCO <sub>3</sub> , TiO <sub>2</sub> , Nd <sub>2</sub> O <sub>3</sub> , Al <sub>2</sub> O <sub>3</sub>	NdAlO <sub>3</sub> , CaCO <sub>3</sub> , TiO <sub>2</sub>	CaTiO <sub>3</sub> , Nd <sub>2</sub> O <sub>3</sub> , Al <sub>2</sub> O <sub>3</sub>	CaTiO <sub>3</sub> , NdAlO <sub>3</sub>
Temperature [°C]				
< 1000	$CaCO_3 \rightarrow CaO + CO_2$  $CaO + TiO_2 \rightarrow CaTiO_3$  <i>and/or</i>  $CaCO_3 + TiO_2 \rightarrow CaTiO_3 + CO_2$			
1000 - 1200	$2CaO + 2TiO_2 + 3Nd_2O_3 + 3Al_2O_3 \rightarrow 2Nd_2TiO_5 + 2CaNdAl_3O_7$  <i>and/or</i>  $2CaTiO_3 + 3Nd_2O_3 + 3Al_2O_3 \rightarrow 2Nd_2TiO_5 + 2CaNdAl_3O_7$  $Nd_2O_3 + Al_2O_3 \rightarrow NdAlO_3$  $Nd_2TiO_5 + CaNdAl_3O_7 \rightarrow CaTiO_3 + 3NdAlO_3$		$2CaTiO_3 + 3Nd_2O_3 + 3Al_2O_3 \rightarrow 2Nd_2TiO_5 + 2CaNdAl_3O_7$  $Nd_2O_3 + Al_2O_3 \rightarrow NdAlO_3$  $Nd_2TiO_5 + CaNdAl_3O_7 \rightarrow CaTiO_3 + 3NdAlO_3$	
>1200	$CaTiO_3 + NdAlO_3 \rightarrow (Ca,Nd)(Ti,Al)O_{3ss}$			



**Figure 6.** (a) Microstructure of the 0.7CaTiO<sub>3</sub>-0.3NdAlO<sub>3</sub> ceramics sintered at 1350 °C/10 h and thermally etched at 1270 °C/10 min. Arrows mark the hexaluminate inclusions. (b) Bright-field TEM image of the hexaluminate inclusion collected along [11·0] zone axis.

reaction layer of the diffusion couple are of the same type as those found in the microstructure of the 0.7CaTiO<sub>3</sub>-0.3NdAlO<sub>3</sub> ceramics. Furthermore, Figure 8 reveals the enhanced growth rate of the CaTiO<sub>3</sub> grains in the vicinity of the reaction layer of the diffusion couple.

The analysis of the regions near the grain boundaries on both CaTiO<sub>3</sub> and NdAlO<sub>3</sub> sides of the diffusion couple are consistent with the results of the EDS analysis of the *continuous phase*. On the CaTiO<sub>3</sub> side the concen-

tration of Nd in the reaction layer formed along the grain boundaries exceeds the concentration of Al. On the other hand, the grain boundaries on the NdAlO<sub>3</sub> side of the diffusion couple contain more Ti than Ca. These results suggest that during the interaction among the perovskites the diffusion of Al from the NdAlO<sub>3</sub> toward the CaTiO<sub>3</sub> is slower than the diffusion of Nd. Consequently, Al predominantly segregates in the form of Al-rich particles. Since these particles are based on hexalu-

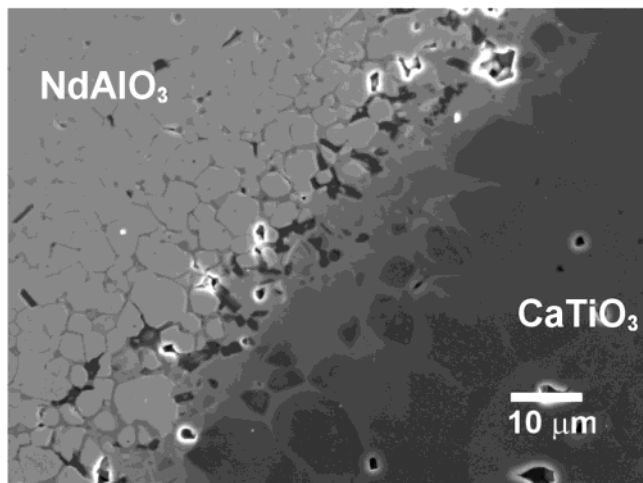


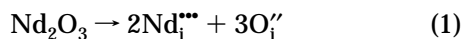
**Figure 7.** CaTiO<sub>3</sub>-NdAlO<sub>3</sub> diffusion couple fired at 1350 °C/6 h.

minate-CaAl<sub>12</sub>O<sub>19</sub>, their formation also consumes some Ca, which is the reason for its lower concentration in the grain-boundary reaction layer formed on the NdAlO<sub>3</sub> side.

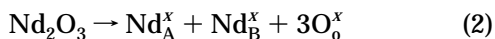
The diffusion couple simulates the situation that occurs at the interface area between CaTiO<sub>3</sub> and NdAlO<sub>3</sub> grains in the reaction mixture during the synthesis of the 0.7CaTiO<sub>3</sub>-0.3NdAlO<sub>3</sub> solid solution. The reaction between CaTiO<sub>3</sub> and NdAlO<sub>3</sub>, apart from the formation of the perovskite solid solution, also results in the nucleation of the CaAl<sub>12</sub>O<sub>19</sub>-based inclusions. A relatively low concentration of these inclusions in the microstructure of the sintered 0.7CaTiO<sub>3</sub>-0.3NdAlO<sub>3</sub> ceramics suggests that they are a transient phase that forms due to kinetic rather than thermodynamic reasons. Thus, the last step in the reaction sequence, which leads to the stoichiometric solid solution, must be the reaction between the CaAl<sub>12</sub>O<sub>19</sub>-based inclusions and the newly formed perovskite phase. Therefore, the concentration of the inclusions in the microstructure of the sintered ceramics depends on the completeness of this solid-state reaction during the calcination process.

The consequence of the presence of the Al-rich CaAl<sub>12</sub>O<sub>19</sub>-based inclusions is the deficiency of Al in the perovskite matrix phase, which necessarily leads to the formation of defects. Since the 0.7CaTiO<sub>3</sub>-0.3NdAlO<sub>3</sub> solid solution is based on the equimolar substitution of Ca with Nd on the A-site and Ti with Al on the B-site, the deficiency of Al in the structure is, in terms of defect chemistry, equivalent to an excess of Nd. Theoretically, there are several different ways to accommodate the excess Nd in the perovskite structure (To satisfy electrical neutrality, the incorporation of Nd into the perovskite matrix must be accompanied by the incorporation of O):

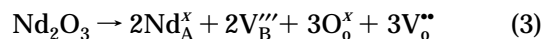
(I) Nd can incorporate into the perovskite interstitially:



(II) Nd can simultaneously occupy A and B sites in the perovskite structure:



(III) Nd can incorporate solely on the A-site, thus creating B-site and oxygen sublattice vacancies:



Since the perovskite structure forms the cubic close-packing arrangement, the formation energies of Frenkel defects are considerably higher than the formation energies of Schottky defects.<sup>13</sup> The incorporation of excess Nd into the interstices according to eq 1 is thus unlikely to occur.

However, the mechanisms for the incorporation of an excess, large A cation, described by eqs 2 and 3, have both been reported in the literature.<sup>14,15</sup> The simultaneous incorporation of excess Nd on A- and B-sites, described by eq 2, would increase the ionic radii difference ( $r_{\text{Nd}^{3+}} = 0.983 \text{ \AA}$ ,  $r_{\text{Ti}^{4+}} = 0.605 \text{ \AA}$ ,  $r_{\text{Al}^{3+}} = 0.535 \text{ \AA}$ , for the coordination number 6)<sup>16</sup> on the B-site and thus increase the distortion of the crystal lattice.

The mode of incorporation of excess Nd as described by the eq 3 leads to the formation of vacancies. Both mechanisms are thus possible sources of the extrinsic dielectric losses.

The mechanism of the accommodation of excess Nd in the perovskite matrix can be inferred from the diffusion couple shown in Figure 8. The micrograph of the etched surface reveals that the CaTiO<sub>3</sub> grains in the vicinity of the reaction layer grow faster than those in the bulk. The EDS analysis shows that the near-grain-boundary area of these grains contains some Nd. Such a situation implies that the incorporation of excess Nd creates high-diffusivity paths along the grain-boundary regions, which increase the grain-growth kinetics. The increase in diffusivity can be attributed to the creation of vacancies in the reaction layer formed along the grain boundaries. The effect of increased grain-growth kinetics due to the formation of oxygen vacancies in the perovskite lattice has already been reported for the case of Nd<sub>2</sub>O<sub>3</sub>-doped BaCeO<sub>3</sub> ceramics.<sup>17,18</sup>

Therefore, the most probable mechanism of accommodating excess Nd in the perovskite structure of the forming solid solution is that described by eq 3. Such a mechanism is further confirmed by the variation of the lattice parameter of the perovskite matrix as a consequence of a different concentration of hexaluminate inclusions, which is discussed in the following text.

In the scope of further experiments we explored the possibility of minimizing the concentration of inclusions by varying the calcination conditions. Figure 9 shows the microstructures of the sintered ceramics based on 0.7CaTiO<sub>3</sub>-0.3NdAlO<sub>3</sub> solid solutions that underwent different calcination procedures. The microstructure shown in Figure 9a belongs to a ceramic based on the 0.7CaTiO<sub>3</sub>-0.3NdAlO<sub>3</sub> solid solution, which was calcined in the form of pellets at 1300 °C/30 h with several intermediate crushings and repelletizings. Figure 9b,

(13) Lewis, G. V.; Catlow, C. R. A. *J. Phys. Chem. Solid* **1986**, *47*, 89.

(14) Desu, S. B.; O'Bryan, H. M. *J. Am. Ceram. Soc.* **1985**, *68* (10), 546.

(15) Han, Y. H.; Appleby, J. B.; Smyth, D. M. *J. Am. Ceram. Soc.* **1987**, *70* (2), 96.

(16) Shannon, R. D. *Acta Crystallogr.* **1976**, *A32*, 751.

(17) Lu, C.-H.; Jonghe, L. C. *J. Am. Ceram. Soc.* **1994**, *77* (10), 2523.

(18) Makovec, D.; Samardžija, Z.; Kolar, D. *J. Am. Ceram. Soc.* **1997**, *80* (12), 3145.

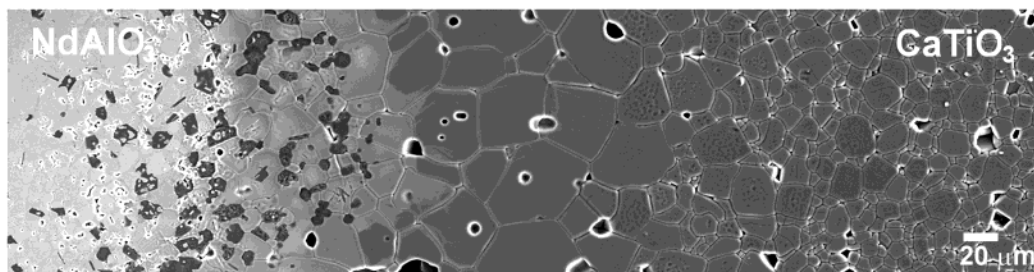


**Figure 8.** CaTiO<sub>3</sub>-NdAlO<sub>3</sub> diffusion couple fired at 1350 °C/100 h, thermally etched at 1300 °C/10 min.

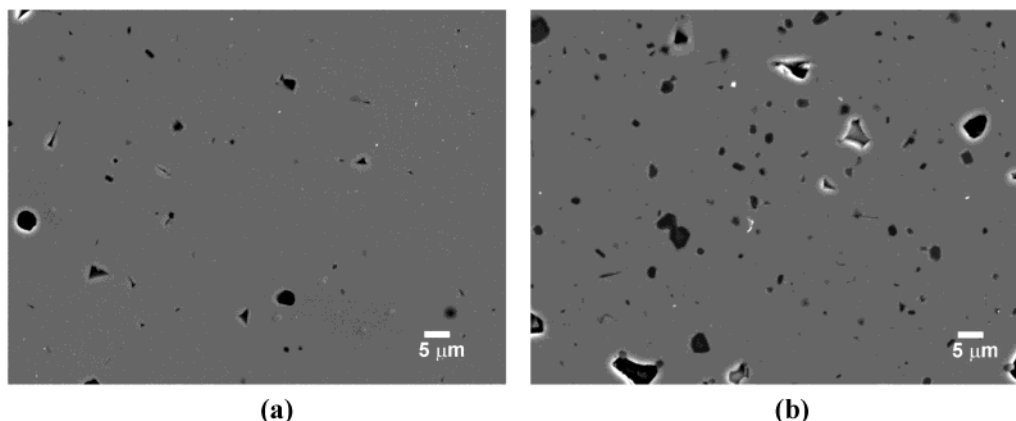


**Figure 9.** Microstructure of the 0.7CaTiO<sub>3</sub>-0.3NdAlO<sub>3</sub> ceramics sintered at 1350 °C/10 h, calcined at (a) 1300 °C/10 h and (b) 1300 °C/30 h with intermediate homogenization.

**Table 2. Lattice Parameters of the Orthorhombic Perovskite 0.7CaTiO<sub>3</sub>-0.3NdAlO<sub>3</sub> Solid Solution vs Calcinations Conditions**

lattice parameters	calcination conditions	
	1300 °C/10 h	1300 °C/30 h
<i>a</i>	5.4040(9)	5.4082(9)
<i>b</i>	7.6188(9)	7.6259(9)
<i>c</i>	5.3784(9)	5.3823(9)

on the other hand, shows the microstructure of a sintered ceramic based on a solid solution calcined at 1300 °C/10 h without intermediate crushing and pelletizing. As can be seen from Figure 9, such a difference in the calcination conditions results in a different amount of hexaluminate inclusions in the microstructure of the sintered ceramic. A less thorough, single-step calcination at 1300 °C/10 h yields a higher concentration of inclusions in the microstructure of the sintered ceramics.

The calculation of the lattice parameters shows that the increased concentration of the residual hexaluminate phase, which is a consequence of a less thorough calcination, results in a decrease of the unit-cell size of the orthorhombic perovskite solid solution (Table 2). In the case of the accommodation of excess Nd in the CaTiO<sub>3</sub>-NdAlO<sub>3</sub> solid solution, such an effect can only be attributed to the formation of vacancies in the crystal structure, which confirms the mechanism described by eq 3.

Table 3 further reveals that a less thorough calcination results in ceramics with a lower Q-value. Such an adverse affect on the Q-value could theoretically be the consequence of either the lossy nature of the hexaluminate phase or the defects in the perovskite matrix associated with its formation. Since the Q-value we measured for the pure CaAl<sub>12</sub>O<sub>19</sub> ceramics sintered at

**Table 3. Microwave Dielectric Properties of the 0.7CaTiO<sub>3</sub>-0.3NdAlO<sub>3</sub> Ceramics Sintered at 1350 °C/10 Hours vs Calcinations Conditions**

calcination conditions	ε <sub>r</sub>	Qxf [GHz]	τ <sub>f</sub> [ppm/K]
1300 °C/10 h	43	27.000	+3
1300 °C/30 h	43	34.000	+3

1600 °C/10 h is relatively high (Qxf = 17000 GHz), we concluded that the major effect arises from the defects formed in the perovskite matrix.

Annihilation of the defects proceeds via a relatively slow solid-state reaction between the hexaluminate inclusions and the perovskite matrix phase. Therefore, to minimize their concentration, time-consuming calcination procedures need to be undertaken (Table 2), which is inconvenient for industrial applications. To shorten the calcination time required for the improvement of the Q-value, we considered adding excess Al<sub>2</sub>O<sub>3</sub> for the synthesis of the 0.7CaTiO<sub>3</sub>-0.3NdAlO<sub>3</sub> solid solution. The excess Al<sub>2</sub>O<sub>3</sub> results in a higher concentration of the hexaluminate inclusions, which increases the contact area between the inclusions and the matrix phase and thus speeds up the reaction. The addition of 3 wt % of Al<sub>2</sub>O<sub>3</sub> prior to calcination at 1300 °C for 10 h results in an increase of the Q-value of the sintered ceramics to Qxf = 39000 GHz, despite a higher concentration of the hexaluminate inclusions in the microstructure.

## Conclusion

The solid-state reaction mechanism that occurs during the synthesis of the 0.7CaTiO<sub>3</sub>-0.3NdAlO<sub>3</sub> solid solutions proceeds via the formation of the perovskite phases CaTiO<sub>3</sub> and NdAlO<sub>3</sub>, regardless of the combination of the oxide powders used as reagents. The two



perovskites react above 1200 °C to form a solid solution. During this reaction the kinetics of the incorporation of Al into the forming perovskite solid solution is slower than the incorporation of Nd, which results in the formation of an Al-rich intermediate phase based on hexaluminate-CaAl<sub>12</sub>O<sub>19</sub>. The last solid-state reaction, which leads to the formation of the single-phase CaTiO<sub>3</sub>-NdAlO<sub>3</sub> solid solution, takes place between the perovskite matrix and the inclusions of the hexaluminate phase. In the case of incomplete calcination some of the CaAl<sub>12</sub>O<sub>19</sub>-based inclusions remain present in the microstructure of the ceramics after sintering. Consequently, excess Nd needs to be accommodated in the perovskite matrix, which leads to the formation of B-site and oxygen sublattice vacancies. Such a defect structure increases the extrinsic dielectric losses (lowers the Q-value) of the CaTiO<sub>3</sub>-NdAlO<sub>3</sub> ceramics. The minimization of the concentration of vacancies, which is necessary for an increase in the Q-value, can be achieved either by a thorough calcination process at temperatures

above 1300 °C involving several intermediate homogenizations of the reaction mixture or by the addition of excess Al<sub>2</sub>O<sub>3</sub> prior to a single-step calcination. A thorough calcination with intermediate homogenizations of stoichiometric amounts of reagent powders allows more time for the reaction between the inclusions and the matrix phase. It thus results in a lower concentration of hexaluminate inclusions in the microstructure and consequently a lower concentration of vacancies in the crystal structure of the perovskite matrix. The use of excess Al<sub>2</sub>O<sub>3</sub> results in a higher concentration of hexaluminate inclusions, which provides an increased contact area between the matrix phase and the inclusions, and thus results in a faster annihilation of the defects in the perovskite. Since the CaAl<sub>12</sub>O<sub>19</sub> is a low-loss phase, the increased concentration of the inclusions itself, as a result of the excess Al<sub>2</sub>O<sub>3</sub>, does not significantly affect the Q-value.

CM034972S